JNeurosci
THE JOURNAL OF NEUROSCIENCE

Research Articles: Behavioral/Cognitive

The Sync/deSync model: How a synchronized hippocampus and a de-synchronized neocortex code memories

George Parish[1], Simon Hanslmayr[2] and Howard Bowman[1,2]

[1]*School of Computing, University of Kent, Canterbury, United Kingdom*
[2]*School of Psychology, University of Birmingham, Birmingham, United Kingdom*

DOI: 10.1523/JNEUROSCI.2561-17.2018

Received: 7 September 2017

Revised: 9 January 2018

Accepted: 7 February 2018

Published: 27 February 2018

Author contributions: G.P., S.H., and H.B. designed research; G.P. performed research; G.P. analyzed data; G.P., S.H., and H.B. wrote the paper.

Conflict of Interest: The authors declare no competing financial interests.

This research was funded by the ERC grant Code4Memory (Grant Agreement 647954) awarded to SH.

Address correspondence to Simon Hanslmayr (s.hanslmayr@bham.ac.uk)

Cite as: J. Neurosci ; 10.1523/JNEUROSCI.2561-17.2018

The Sync/deSync model: How a synchronized hippocampus and a de-synchronized neocortex code memories

George Parish[1], Simon Hanslmayr[2,*], Howard Bowman[1,2]

1: School of Computing, University of Kent, Canterbury, United Kingdom

2: School of Psychology, University of Birmingham, Birmingham, United Kingdom

* Address correspondence to Simon Hanslmayr (s.hanslmayr@bham.ac.uk)

Number of Figures: 8

Number of Words:

- Abstract: 244
- Significance Statement: 120
- Introduction: 650
- Discussion: 1493

Acknowledgements: This research was funded by the ERC grant Code4Memory (Grant Agreement 647954) awarded to SH.

Abstract

Neural oscillations are important for memory formation in the brain. The de-synchronisation of Alpha (10Hz) oscillations in the neo-cortex has been shown to predict successful memory encoding and retrieval. However, when engaging in learning, it has been found that the hippocampus synchronises in Theta (4Hz) oscillations, and that learning is dependent on the phase of Theta. This inconsistency as to whether synchronisation is 'good' for memory formation leads to confusion over which oscillations we should expect to see and where during learning paradigm experiments. This paper seeks to respond to this inconsistency by presenting a neural network model of how a well-functioning learning system could exhibit both of these phenomena, i.e. desynchronization of Alpha and synchronisation of Theta during successful memory encoding.

We present a spiking neural network (the Sync/deSync model) of the neo-cortical and hippocampal system. The simulated hippocampus learns through an adapted spike-time dependent plasticity rule, in which weight change is modulated by the phase of an extrinsically generated Theta oscillation. Additionally, a global passive weight decay is incorporated, which is also modulated by Theta phase. In this way, the Sync/deSync model exhibits Theta phase-dependent long-term potentiation and long-term depression. We simulated a learning paradigm experiment and compared the oscillatory dynamics of our model with those observed in single-cell and scalp-EEG studies of the medial temporal lobe. Our Sync/deSync model suggests that both the de-synchronisation of neo-cortical Alpha and the synchronisation of hippocampal Theta are necessary for successful memory encoding and retrieval.

Significance Statement

A fundamental question is the role of rhythmic activation of neurons, i.e. how and why their firing oscillates between high and low rates. A particularly important question is how oscillatory dynamics between the neo-cortex and hippocampus support memory formation. We present a spiking neural-network model of such memory formation, with the central ideas that 1) in neo-cortex, neurons need to break-out of an Alpha oscillation in order to represent a stimulus (i.e. Alpha desynchronises), while 2) in hippocampus, the firing of neurons at Theta facilitates formation of memories (i.e. Theta synchronises). Accordingly, successful memory formation is marked by reduced neo-cortical Alpha and increased hippocampal Theta. This pattern has been observed experimentally and gives our model its name – the Synch/deSynch model.

Introduction

Brain oscillations, via their ability to synchronize and desynchronize neuronal populations, play a crucial role in the formation and retrieval of episodic memories. However, little is known about how oscillations implement the necessary mechanisms for encoding and retrieval of such memories. This knowledge gap is partly due to a lack of computational models simulating oscillatory behaviours as observed in human EEG/MEG recordings during memory tasks. The link between oscillations and memory is further complicated by empirical data, which has fuelled a conundrum as to how oscillations relate to memory. Specifically, hippocampal Theta (~3-8 Hz) and gamma (~40-80 Hz) synchronisation (Fell & Axmacher, 2011) and the de-synchronisation of Alpha and beta (8-30 Hz) in cortical regions (Hanslmayr, et al., 2012) have both been reported as important for memory encoding and retrieval. Classic computational models theorise that hippocampal and neo-cortical regions offer functionally distinct mechanisms to form episodic memory (O'Reilly, et al., 2014), where a sparsely connected hippocampus learns new information quickly and a dense neo-cortex incorporates this information slowly. Building on these complementary learning systems, we recently presented a potential solution to the synchronization/de-synchronization conundrum (Hanslmayr, et al., 2016), suggesting that hippocampal Theta synchronisation (~4Hz) mediates the binding of concepts, while neocortical Alpha de-synchronisation (~10Hz) is due to the representations of these concepts becoming active. We here present a first computational network model which implements these mechanisms and simulates the opposing synchronizing and desynchronizing behaviours in the hippocampus and neocortex during a typical episodic memory task. Our model, while being very simple, successfully simulates a number of empirical findings ranging from human single neuron recordings, intracranial EEG recordings, to non-invasive EEG/MEG recordings and therefore represents a useful theoretical link between different levels of human electrophysiological recordings.

Theta oscillations in medial temporal lobe are assumed to play a key role in the formation of memories, where learning is dependent on the power of Theta oscillations and the timing of action

92 potentials in relation to the ongoing Theta cycle (Rutishauser, et al., 2010) (Backus, et al., 2016)
93 (Staudigl & Hanslmayr, 2013) (Heusser, et al., 2016). Studies in rodents have provided a mechanism
94 by which Theta oscillations exert their influence on memory in showing that Long-Term-Potentiation
95 (LTP) and Long-Term-Depression (LTD) occur in specific phases of the Theta cycle (Huerta & Lisman,
96 1995) (Pavlides, et al., 1988). Building on theories of synaptic plasticity, it has been postulated that
97 LTD occurs whilst most neurons in region CA1/CA3 are active in the excitatory phase of Theta (as
98 recorded from CA1/CA3 hippocampal regions), whereas LTP occurs in the inhibitory phase of Theta
99 when most neurons are silent (Hasselmo, 2005). (We clarify how these inhibitory and excitatory
100 phases map onto the trough and peak of Theta in subsection "Computational model"). The model we
101 describe here shows that stimulated hippocampal cells demonstrate a phase shift forward in Theta,
102 enabling LTP to occur in the inhibitory phase of Theta where other non-stimulated cells are silent.

103 Concerning Alpha oscillations, it can be assumed that there is a negative relationship between Alpha
104 power and discriminating neural activity (Haegens, et al., 2011), leading to the notion that Alpha
105 provides functional inhibition (Klimesch, et al., 2007) (Jensen & Mazaheri, 2010). Supporting this
106 notion, Alpha power decreases (i.e. desynchronizations) are often localized in cortical regions relevant
107 for a given task, whereas Alpha power increases occur in competing areas that are being inhibited
108 (Jokisch & Jensen, 2007) (Waldhauser, et al., 2012). These findings suggest that the de-synchronisation
109 of Alpha represents the flow of information to a targeted group of neurons. Consistent with this
110 general gating function of Alpha, power decreases are strongly evident in episodic memory tasks
111 where cortical Alpha power decreases predict successful encoding (Hanslmayr, et al., 2012) and
112 retrieval (Khader, et al., 2010) (Waldhauser, et al., 2016). In addition to the hippocampal Theta
113 dynamics, our model also simulates such memory dependent Alpha power decreases in the neocortex
114 during the encoding and retrieval of episodic memories.

115

116

Materials and methods

Computational model

Here we describe a simple computational neural network model, which takes inspiration from the complementary learning systems framework (CLS), and lends credence to the previously theorised notion that opposing oscillatory behaviour in cortical and Hippocampal regions both contribute to episodic memory formation (Hanslmayr, et al., 2016). We do not fully detail the different steps of how information enters and exits the hippocampus through different subregions, e.g. via the perforant pathway from entorhinal cortex. Importantly, Theta oscillations show a phase reversal between the two pathways from entorhinal cortex to CA1 (the monosynaptic perforant pathway and the tri-synaptic pathway, via the schaffer collaterals), which is the focus of previous models describing the computational utility of Theta in providing discrete time windows for encoding and retrieval (Hasselmo et al., 2005) or error-driven learning (Ketz et al., 2013). Our model draws inspiration from these works, but focusses particularly on the dynamics in region CA1. The key functional property we have constructed our model upon is that Theta sets up an inhibitory phase at the soma of pyramidal cells, at which LTP occurs, and a facilitatory phase at the soma of such cells, at which LTD occurs. Neurophysiologically, this could arise from the coincidence of a trough of fissure Theta (which is known to coincide with LTP); a peak at stratum radiatum (input from schaffer collaterals to CA1); and a trough at stratum pyramidale (i.e. functional inhibition at the cell body). This pattern is justified in (Hasselmo et al., 2005, section “Induction of LTP”), and is consistent with (Hanslmayr, et al., 2016), which refers to the peak in stratum radiatum. To simplify presentation, through the main body of the paper, we use functional descriptors, i.e. we talk in terms of the inhibitory phase of Theta, meaning functional suppression at the pyramidal cell body, and the facilitatory phase of Theta, meaning functional facilitation at the pyramidal cell body. In these terms, we will model a simple mechanism to simulate a typical episodic memory paradigm where an association between stimuli has to be learnt

in one trial. A principle of our modelling endeavour has been to identify the simplest neural instantiation of our theory under an Ockham's razor principle.

Experimental paradigm

We chose to compare our model to an experiment that recorded from medial-temporal-lobe (MTL) neurons within epilepsy patients (Ison, et al., 2015). As depicted in Figure 1A, the experimenters screened many images of people to each participant to find one that the neuron under observation responded to, denoted from here on as the preferred (P) image. A separate image of a location was chosen that the neuron did not respond to, denoted as the non-preferred (NP) image. The P image of the person was then digitally superimposed onto the NP image of the location (denoted here as the composite (C) image), before being presented to the participant in what is termed here as the learning phase. The experimenters then conducted the screening process again, presenting both the NP & P images, to assess the impact of learning on the activity of the Hippocampal neuron. Figure 1A shows how we simulated this paradigm, where there is a screening phase before and after the presentation of the composite stimulus.

Neuron physiology

Our model comprises two groups of neurons representing the neo-cortex (NC) and the hippocampus (Figure 1Ba), split again into two subgroups coding for the P and NP images (where the number of neurons in each group was $N_{NC} = 20, N_{hip} = 10$). All neurons are simulated using an Integrate-and-Fire equation ($equation\ 1$, $V_{th} = -55mV$, $E = -70mV$, $C_m = 240nF, V_{ref} = 2ms, \tau_m = 20ms$). A spike event is sent to other downstream connected neurons if the membrane potential ($V_m(t)$) of a neuron surpasses the threshold for firing (V_{th}). After a spike, the neuron enters a refractory period, where the membrane potential is clamped to the resting potential (E) for a set period (V_{ref}). With this equation, the membrane potential of a neuron is constantly decaying to its resting potential (E) at a rate dictated by the membrane time constant (τ_m). The sum of all inputs at t is divided by the capacitance (C_m) of the membrane potential. Inputs originate from constant alternating currents

(I_{tonic}), the sum of excitatory-post-synaptic-potentials (EPSPs) from spikes at each input synapse (I_{syn}) and an after-de-polarisation function (I_{ADP}), which will be described in more detail later.

$$\Delta V_m(t) = \frac{E - V_m(t-1)}{\tau_m} + \frac{I_{tonic}(t) + I_{syn}(t) + I_{ADP}(t)}{C_m}$$

Equation 1: The integrate-and-fire model

An Alpha function ($equation\ 2$) was used to model EPSPs for incoming spike events, where Δt is equal to the current time (t) minus the time of the eliciting spike (t_{fire}). The higher the synaptic time constant τ_s, the larger the integral through time of the EPSP, ensuring that a spike has a more sustained effect on the receiving neuron's membrane potential. All synapses within the NC integrated with a τ_s of 1.5ms, whilst synapses within the Hippocampus integrated with a slightly larger synaptic time constant ($\tau_s = 5ms$) to allow them to more easily interact with one another. Spikes originating from external noise generators had a synaptic time constant of $1.5ms$.

$$EPSP(t) = \left(e \cdot \frac{\Delta t}{\tau_s}\right) \cdot \exp\left(-\frac{\Delta t}{\tau_s}\right), \qquad \Delta t = t - t_{fire}$$

Equation 2 : The Excitatory-Post-Synaptic-Potential (EPSP)

Neocortical system

Based on CLS, the NC system learns slowly from repeated presentations. As our model emphasises the effect of oscillations on a single learning event, we assumed the existence of two pre-established NC populations, one representing the P and the other the NP concept, where neurons within each population had a 25% chance of being connected and synaptic modification was not implemented due to an assumed slow cortical learning rate (Figure 1Bi). Each NC neuron received background noise, representing "chatter" from other brain regions, in the form of Poisson distributed spike-events (~42k spikes/s). We do not explicitly model a neural mechanism for oscillations, thus a cosine wave of frequency 10Hz (amplitude = 21pA) was fed into NC neurons via I_{tonic} to model ongoing Alpha. This approximates the dominance of Alpha oscillatory activity in the cortex, which arise via pacemaker

regions like the thalamus (Hughes, et al., 2004) or emerge via cortico-cortical top-down interactions (van Kerkoerle, et al., 2014). Two separately generated Poisson distributed spike-trains (~80k spikes/s) were then paired with each NC subgroup upon stimulus presentation, modelling the activation of the P and/or NP images from higher cortical and visual areas. Stimulus related spike-trains were multiplied by an Alpha function (equation 2, τ_s = 250ms) to more realistically model the activation of many neurons at stimulus onset.

Hippocampal system

Hippocampal neurons were similarly organised into two subgroups (Figure 1Bi), where each neuron received background noise (~4k spikes/s) and a cosine wave of 4Hz (amplitude = 28pA) to model ongoing Theta. This ongoing Theta oscillation approximates input into the hippocampus from pacemaker regions like the septum (Petsche, et al., 1962), or interactions between different types of interneurons acting as local Theta generators (Rotstein, et al., 2005). Based on CLS, the Hippocampal system learns quickly from a single presentation. Therefore, Hippocampal synaptic modification was enabled via an adapted Spike-Time-Dependent-Plasticity (STDP) learning rule (Song, et al., 2000). We adjusted this rule to relate to empirical evidence that Hippocampal learning is Theta phase dependent (Huerta & Lisman, 1995), with LTP occurring in the functionally inhibitory phase and LTD in the functionally excitatory phase of Theta (Hasselmo, 2005). To this end, synaptic LTP was implemented by multiplying STDP weight modifications by the phase of the Theta cosine wave, with a value between 0 and 1, with 0 on the excitatory "up" phase and 1 on the inhibitory "down" phase (Figure 1Bii).

When a neuron spiked, a reward (A_+) for contributing synapses was calculated as the product of a constant learning rate ($\varepsilon \in \mathbb{R}. 0 \leq \varepsilon \leq 1$), Theta at time t ($\theta \in \mathbb{R}. 0 \leq \theta \leq 1$) and the maximum weight (W_{max}), whilst punishments for competing synapses were calculated as $A_- = 1.1 \cdot A_+$ ($equation\ 3$). The greater strength for A_- compared to A_+ reflected a preference for synaptic weakening in order to maintain a stable network. Whenever a spike event occurs, at unit i or j, an

accumulated STDP update $v_{ij}(t)$ for synapse i to j is calculated from its history of previous spiking (i then j or j then i) ($equation\ 5$). A function was then used to calculate the STDP acting on the synapse ($equation\ 4$), where an exponential weighting of A_+ was applied if the pre-synaptic spike occurred before the post-synaptic spike and of A_- if the post-synaptic spike occurred first. All Hippocampal weights were subject to STDP updates, along with an exponential passive decay, which was multiplied by the complement of the phase of Theta $(1-\theta(t))$ ($equation\ 6$). The presence of this decay is consistent with the non-specific LTD that might occur during oscillatory spiking in the facilitatory phase of Theta (Hasselmo, 2005). This decay was larger for smaller weights, establishing a transition point whereby weakly interacting synapses were pruned ($\tau_w = 20$). A piecewise linear bounding function was used to protect against sign reversal and run-away weights ($equation\ 7$; $W_{max} = 120$; $W_{min} = 0$).

$$A_+ = \varepsilon \cdot \theta(t) \cdot W_{max}, \qquad A_- = 1.1 \cdot A_+$$

Equation 3 : Reward (A_+) and punishment (A_-) of synapses.

$$F(\Delta t) = \begin{cases} A_+ \cdot \exp(\Delta t/\tau_s), & if\ \Delta t < 0 \\ -A_- \cdot \exp(-\Delta t/\tau_s), & if\ \Delta t \geq 0 \end{cases}$$

Equation 4 : Function for STDP between pre and post-synaptic spikes (Song, et al., 2000), where Δt is always the difference between the time of a pre-synaptic and post-synaptic spike.

$$\forall i, j \in \aleph\ s.t.\ C(i,j)\ .$$

$$v_{ij}(t) = \begin{cases} \sum_{t' \in T(i,t)} F(t'-t), & if\ S(t)_j \\ \sum_{t' \in T(j,t)} F(t-t'), & if\ S(t)_i \\ 0, & otherwise \end{cases}$$

$$T(k,t) = \{\, d \in \mathbb{R}^{0,+} \mid S(d)_k \wedge t \geq d \,\}$$

Equation 5 : SDTP synaptic modification at time t for a network with node labels $\aleph = \{1, \dots, n\}$. $C(i,j)$ is true if and only if i and j are connected. $S(t)_i$ indicates a spike event at the ith neuron at time t. $T(k,t)$ returns the set of all times before time t, at which there was a spike at neuron k. This is used to provide spike events paired, across synapse i, j, with the spike at time t. In addition, we use auxiliary weight variables v_{ij} and V_{ij} to enable application of a piecewise linear bounding function, see eqn 7.

$$\forall i,j \in \aleph \; s.t. \; C(i,j) \;\; . \;\; V_{ij}(t) = W_{ij}(t-1) + v_{ij}(t) - \frac{(1-\theta(t)) \cdot \exp\left(-\frac{W_{ij}(t-1)}{\tau_w}\right)}{\tau_w}$$

Equation 6 : Update of auxiliary weight variable and implementation of non-specific passive decay of synapses.

$$W_{ij}(t) = \begin{cases} W_{min}, & if \; V_{ij}(t) < W_{min} \\ W_{max}, & if \; V_{ij}(t) > W_{max} \\ V_{ij}(t), & otherwise \end{cases}$$

Equation 7 : Piecewise linear bounding function

Hippocampal neurons were interconnected with a probability of 40% to form a connection. Additionally, as it was assumed that both images were previously known to the participants but not associated, a random 50% of synapses within each subgroup had initial synaptic weights of W_{max} whilst all others were set to 0. This ensured the random assignment of pre-established sets of winning and losing pathways within the subgroups coding for the P & NP image.

Hippocampal neurons received additional input from an After-De-Polarisation (ADP) function (Jensen, et al., 1996) to control activation ($equation\ 8$; $A_{ADP} = 100pA, \tau_{ADP} = 250ms$). This provided exponentially ramping input, which was reset after each spike-event (t_{fire}). Evidence for an ADP function in hippocampal neurons has been found experimentally during cholinergic (Andrade, 1991)

(Caesar, et al., 1993) (Libri, et al., 1994) and serotonergic (Araneda & Andrade, 1991) modulation, and has the effect here of modelling an effectively inhibitory input for each Hippocampal neuron, which wanes the further one is from the eliciting spike.

$$I_{ADP}(t) = \frac{A_{ADP} \cdot \Delta t}{\tau_{ADP}} \cdot \exp\left(1 - \frac{\Delta t}{\tau_{ADP}}\right), \qquad \Delta t = t - t_{fire}$$

Equation 8 : After-De-Polarisation (ADP) function

Local Field Potential (LFP) and Time Frequency Analysis (TFA) methods

The LFP measures the activity of a group of neurons by first aggregating spikes through time. This was then filtered twice, first by using a Hanning filter with a 30ms window and then again with a sampling frequency between 2-6Hz or 8-12Hz dependent on whether we are filtering by Theta or Alpha, respectively. The LFP was analysed in time-frequency space using a Gabor filter with an upper and lower bound of 2-6Hz or 8-12Hz for Theta or Alpha analysis ($\gamma = 0.5$ for <30Hz or $\gamma = \pi/2$ for >30Hz). The absolute values were then taken and plotted in time-frequency space.

Code Availability

The Matlab code that was used to generate the results in reported in this manuscript can be downloaded at https://github.com/GP2789/Sync-deSync-model.

Results

Simulation procedure

We simulated our model based on a learning paradigm used in an MTL single cell recording experiment (Ison, et al., 2015). During the initial screening phase, both the P & NP images were presented individually. This was simulated by independently creating two Poisson distributed spike trains (~80k/s for 2 seconds) that fed into each respective P & NP subgroup of NC neurons (Figure 1A; P = blue, NP = magenta). An inter-stimulus interval of 2 seconds was used. Afterwards, we presented both images in a composite stimulus (green), where both subgroups of NC neurons concurrently received spike-trains. Following this learning phase, we repeated the screening phase to assess the capability of the network to associate these stimuli together. The whole process was simulated 1000 times to assess the variability of the network, where for each simulation the Alpha and Theta cosine waves each began at a different random phase (choosing a random 30° angle between 0-360°, i.e. $N \times 30° \; where \; N \in \mathbb{N} \; s.t. \; 0 \leq N \leq 12$), new noisy spike trains were generated, and new initial patterns of connectivity were established. Thus, there was no carry-over of weight values between runs. The following results take an average over all simulations, where each simulation is treated as an individual trial with default initial parameters.

Hippocampal weight change

Maximal synaptic modification occurs between Hippocampal neurons that are stimulated to shift forward in phase and fire in the inhibitory cycle of an ongoing Theta oscillation (Hasselmo, 2005). Due to this, synaptic learning only occurs during the screening and learning phases of the simulation (Figure 2; NP stimulus-magenta; P stimulus-blue; C stimulus-green) and not during the inter-stimulus intervals. Weight change after stimulus onset follows the Alpha function shape of the activation fed into these neurons. Due to the maximisation of a random 50% of synapses within each P & NP subgroup, the average weights of these groups begin at $W_{max}/2$ (Figure 2A). Throughout the entire simulation, there is weight change within each subgroup (P-blue line; NP-magenta dash) when the respective image they are coding for is presented. With the competitive STDP rule, winning and losing weights are pushed towards W_{max} or W_{min} respectively, causing a capping effect where a weight in

one direction can still change whilst its competitor is capped. Here, this means that the average weight of each subgroup rises a small amount to stabilise just above $W_{max}/2$ every time the respective image is presented.

When the composite stimulus is presented (green), there is only marked synaptic change between both subgroups (Figure 2B; P->NP-blue line; NP->P-magenta dash). Here, weights go up bi-directionally as both subgroups of neurons are concurrently stimulated to become active during the inhibitory phase of Theta. In this phase, there are short term increases and decreases in weights, as paths are found between subgroups. As indicated by figure 2B, DL period, sustained changes are positive. When the screening phase is repeated after the learning phase, weights fluctuate and eventually settle with an increase in the direction from the active population to the non-active population. Before learning, concepts are only strengthened when the relevant image is presented. After learning, both concepts are reinforced upon the presentation of either image, indicating how previously associated but non-present concepts can remain strong over time.

Weights passively decay very slowly according to an exponential pattern to model the effect of a large population of neurons spiking during the facilitatory phase of Theta, where LTD has been found to occur (Hasselmo, 2005). As LTP occurs over a spectrum of 1 to 0, small weight increases occur as neurons spike on either side of the point at which Theta maximally inhibits. The passive decay implemented here is stronger for smaller weights (equation 6), to mitigate these gradual weight increases and prune irrelevant synapses. This can be seen most prominently in Figure 2B during the initial screening phase (2-4 & 6-8 seconds), where small weight increases to stimulated neurons decay quickly. LTD weight decay is also prominent in the inter-stimulus periods, where all weights slowly reduce over time.

Hippocampal activity

Activity is measured as the sum of spikes within bins of a 20ms width throughout the length of a simulation, taking an average of 1000 simulations with varying random phases for Alpha and Theta

oscillations, where the mean firing rate is shown with bootstrapped confidence intervals (Figure 3A). As we have access to data from both preferred (P) and non-preferred (NP) neurons, we can capture the network's capability of recognition, where P & NP units respond to their own stimulus, and cued recall, where P & NP units respond to the opposite stimulus. During the initial screening phase before learning (BL), we see that neurons respond to their relevant images (Figure 3A), where activation at stimulus onset seems to cause a phase reset. This generates a high-frequency damped oscillation that is phase consistent across replications, and rides on top of a much lower frequency evoked transient, which plays out over a second or more.

When the C image is presented during learning (Figure 3Ci), activity increases dramatically. Figure 3Cii shows the cause of this increase by breaking down the average input coming into neurons during learning, where the sum of all input sources follows the grey area (I). Here, we see an external force (I_{ext}) drive the hippocampus at stimulus onset, which then causes the ADP current (I_{ADP}) to reset before it can reach maximum conductance (*Equation 8;* A_{ADP}), thus reducing its effect. The relative increase in activation is due to substantial weight change, and resulting additional input, between subgroups ($I_{H<>H}$). Activation then feeds back into each subgroup dependent on how weights develop.

When the screening phase is repeated after learning, the network successfully performs cued recall (Figure 3Bii) due to the aforementioned weight change, showing that our model efficiently learns associations between two arbitrary stimuli in one short presentation, a crucial requirement for a model of episodic memory. Similarly, random reciprocal feedback of activity between subgroups causes a relative increase in activation (Figure 3Bi).

Raster plots show the activation of a single random P and NP neuron, as they respond to presentations of the P stimulus through a randomly chosen trial, where each line corresponds to a spike event (Figure 3Aiii, Biii & Ciii). These are colour co-ordinated with the relevant activation plots seen above.

We compare the results of our simulation to those from experimental evidence from a recent human single unit learning paradigm (Ison, et al., 2015). Figure 3Di-ii shows smoothed curves (smoothing

spline; $p = 1e^{-7}$) following simulated recognition and cued recall performance before and after learning, compared to experimental evidence of the same data in Figure 3Diii. Despite some overlap of confidence intervals, Figures 3Di-ii suggest that there is an increase in pre-stimulus activation after learning for recognition and recall in both sets of data. Raster plots show that this could be caused by occasional double spike events during the excitatory phase of Theta, due to increased weights between neurons (Figure 3Biii; -500 to 0ms). Both the model and experimental data indicate successful cued recall after learning (Figure 3Dii/iii; green), however, recognition after learning varies (Figure 3Di/iii; red). The experimental finding is that encoding neurons become less active with successive presentations of the same stimulus (Ison, et al., 2015), perhaps due to a repetition suppression effect (Pedreira, et al., 2010). In our model, an increase in recognition activation after learning is caused by the overall increase in synaptic efficacies both between and within subgroups. This could be countered by implementing a habituation mechanism that lies outside of the scope of this model. Such a mechanism could involve the re-balancing of weights or the storing of short-term-memory in a higher brain structure.

Theta phase

Figure 4 shows Theta phase for the cued recall condition during the 3 stages of the simulation. The red and green halves of the polar distribution represent the excitatory and inhibitory phases of the 4 Hz cosine wave used to model Theta, where π/2 is maximum excitation and -π/2 is maximum inhibition. The total number of spikes occurring within each phase quadrant of Theta was recorded (Figure 4Ai, Bi & Ci), as well as the first spike of each neuron after maximum inhibition (>-π/2) (Figure 4Aii, Bii & Cii). The latter analysis was performed to show how Hippocampal neurons shift forward in Theta phase once stimulated. Spike numbers were normalised over 1000 simulations.

Before learning, neurons are un-responsive to the image they do not encode for and oscillate at Theta, where all spikes occur during the excitatory phase (Figure 4Ai 0 to π/2 to π), with the first spikes generally occurring just before maximum excitation (Figure 4Aii; 0 to π/2). When the C image is

375 presented during the learning phase, both subgroups become active across all phases of Theta (Figure
376 4Bi). Importantly, in order for activation to overcome inhibition, more activity will occur during the
377 inhibitory phase of Theta. Neurons also exclusively spiked first immediately after the inhibitory
378 maximum (Figure 4Bii; -π/2 to 0), indicating that all neurons in the P subgroup successfully phase-
379 shifted forward once stimulated during learning.

380 When the screening phase occurs again after learning, neurons now respond to the opposite image.
381 Spikes occur in most phase quadrants of Theta (Figure 4Ci), but in the main during the excitatory
382 phase. However, inhibition can now be overcome, allowing spikes to first occur during the negative
383 phase of Theta (Figure 4Cii) and demonstrating a phase shift forward in Theta. This shift in phase is an
384 index of successful learning and has been well documented in rodents for neurons encoding a
385 particular place when the rodent approaches that place (Huxter, et al., 2003). Our model shows a
386 similar behaviour and predicts that this shift in phase is responsible for associative memory formation.
387 Importantly, this phase shift is most evident when analysing only the first spike within a Theta cycle,
388 starting at the Theta trough (i.e. where inhibition is maximal). This prediction can be tested in studies
389 recording single units and local field potentials in human epilepsy patients (Ison, et al., 2015).

390 **Alpha De-Synchronisation**

391 Figure 5A shows time-frequency power spectra (8-12Hz) of the LFP of the NC neurons for the recall,
392 recognition and learning phases. A thick band at 10Hz during the recall condition before learning
393 shows non-stimulated neurons oscillating at Alpha (Figure 5Ai), as they do not respond to an image at
394 this time. When neurons are responsive to the image they encode for in recognition and learning
395 conditions, a strong de-synchronisation of Alpha is exhibited (Figure 5Aii/iii/v; 0 to 1s), simulating the
396 well-documented effect of Alpha suppression upon visual stimulation (Berger, 1929). A similar, but
397 weaker effect can be seen in the cued recall condition after learning (Figure 5Aiv; 0 to 1s). This de-
398 synchronisation is due to learning driven activation of Hippocampal neurons caused by the association
399 between the P and NP stimuli. This low-frequency drive (from Hippocampus to Neo-cortex) de-

synchronises Alpha by causing substantial activation in the inhibitory phase. The effect can be more clearly seen in Figure 5Bii, where a 20% relative decrease in Alpha power from pre to post stimulus is exhibited (Figure 5Bii; 0 to 1s), consistent with the findings that memory retrieval can be predicted by this same Alpha de-synchronisation (Hanslmayr, et al., 2012). Pre stimulus Alpha power is also slightly stronger (Figure 5Bi; -1 to 0s), indicating that pre-stimulus Alpha/beta power can be used to predict memory formation (Salari & Rose, 2016). This is due to stronger weights within Hippocampal subgroups causing knock-on activation during the excitatory phase of Alpha. This activation feeds back into Hippocampal units to cause an even more pronounced increase in pre-stimulus Alpha after learning (Figure 5Ci), where after stimulus onset Alpha also significantly decreases in these hippocampal units (Figure 5Cii), which is consistent with a previous study (Staresina, et al., 2016).

This behaviour of our model mimics several findings in the literature showing memory dependent Alpha power decreases during the reinstatement of episodic memories (Khader, et al., 2010) (Waldhauser, et al., 2016) (Michelmann, et al., 2016). Here, the de-synchronisation of Alpha represents the flow of information in the NC caused by activation of relevant stimuli (Jensen & Mazaheri, 2010), (Klimesch, et al., 2007).

Theta Synchronisation

Figure 6Ai-v shows time-frequency power spectra (2-4Hz) of the LFP of Hippocampal neurons for the recall, recognition and learning conditions. In the recall condition before learning, neurons do not respond to any image and oscillate at Theta (Figure 6Ai). An increase in Theta power accompanies increased activation, as neurons respond to the image they encode for before and during learning (Figure 6Aii-iii). Theta synchronisation is stronger during learning, consistent with experimental evidence (Backus, et al., 2016) (Lega, et al., 2012) (Staudigl & Hanslmayr, 2013). This is due to the rapid increase in synaptic weights during this period (Figure 2B; 10 to 12s) causing feedback activation, which, in turn, causes more neurons to fire above threshold, but according to the Theta rhythm.

After the learning phase, neurons are also responsive to the opposite image, where a synchronisation of Theta occurs due to an increase in activity post stimulus (Figure 6Aiv). This can be seen more clearly in Figure 6Bii, where there is up to a 60% increase in Theta power relative to the pre-stimulus period. Due to stronger weights between the P & NP cluster, there is increased feedback activity during the normal oscillatory rhythm. This activity is amplified by a higher synaptic time constant (τ_s = 5ms for hippocampal neurons), causing an increase in pre-stimulus Theta power (Figure 6Bi; -1 to 0s). The same changes in Theta power are passed through to the NC (Figure 6Ci-ii), which is consistent with experimental evidence of increases of Theta in NC areas after learning paradigm experiments (Burke, et al., 2014) (Klimesch, et al., 2005).

Varying Stimulus Strength

We next varied how strongly our simulated participant perceived the P & NP images during the encoding and recall after learning conditions, allowing us to explore the sync/de-sync of Hippocampal Theta and NC Alpha over time at different strengths. This is achieved by varying stimulus strength, i.e. the rate of spikes per second being fed into NC neurons at stimulus onset, and taking the average power during the post-stimulus period across frequencies (0-30Hz). This information is displayed as heatmaps of frequency vs stimulus strength (Figure 7Ai-ii & Di-ii), where stimulus strength is shown on a logarithmic scale from 10^0 to 10^6. We can extract from this information to show the evolution of NC Alpha (Figure 7B; Red, 8-12Hz) and Hippocampal Theta (Blue, 3-5Hz) as neurons are driven more. It can be shown that for weakly perceived stimuli, the NC actually synchronises in Alpha within the model (see around 10^3 strength). This is due to input activity being too weak to overcome the trough of the 10Hz cosine input, but strong enough to cause more spiking in the peak. As stimulus strength increases, a de-synchronisation of Alpha is obtained as neurons overcome inhibition to spike across all phases of Alpha (see around 10^5 strength). In contrast, the Hippocampus exhibits a strong synchronisation of 4Hz (Figure 7B) with increasing stimulus strength. This is due to the ADP function preventing neurons recovering quickly after a spike event. This then is an important difference

449 between the neo-cortical and hippocampal systems, which underlies why (apart from with very strong
450 inputs) the hippocampus synchronises rather than desynchronises – essentially the ADP function
451 prevents the hippocampus from desynchronising. Weight change between P & NP units also increases
452 monotonically with stimulus strength, plateauing at the same level that Theta and Alpha maximally
453 synch/de-sync, respectively. This indicates why Alpha de-synchronisation and Theta synchronisation
454 are both markers of successful memory encoding (Backus, et al., 2016) (Lega, et al., 2012) (Staudigl &
455 Hanslmayr, 2013) (Hanslmayr, et al., 2012). Hippocampal Theta synchronisation can also be seen to
456 bleed into NC neurons as stimulus strength increases (Figure 7Ai; 10^4 to 10^6 strength), corroborating
457 experimental evidence (Burke, et al., 2014) (Klimesch, et al., 2005).

458 When we push the model past normal levels of activation (the model's default is ~$8x10^4$), Hippocampal
459 Theta eventually de-synchronises, indicating that although the ADP function essentially acts as a break
460 on Hippocampal units, it can eventually be overcome. Weight change remains high as units are spiking
461 across all phases of Theta. This gives a possible explanation for why some experimental evidence also
462 finds a positive correlation with successful memory encoding and hippocampal Theta de-
463 synchronisation (Fellner, et al., 2016) (Crespo-Garcia, et al., 2016) (Greenberg, et al., 2015).

464 We also choose three important points from Figure 7B that best convey the model's sync/de-sync
465 characteristics, indicated by vertical green lines during first normal oscillatory behaviour, second,
466 Alpha sync and third, maximal Theta sync and Alpha de-sync. The corresponding LFPs (indicated by
467 the same symbol) are shown for these three points for NC (Figure 7Ci) and Hippocampal units (7Cii).
468 NC Alpha LFPs show how power can increase when more spikes during the excitatory phase cause
469 larger amplitudes of activity (Ci; cross), and how power decreases when activation occurs throughout
470 an oscillation (Ci; triangle). Similarly, Hippocampal Theta LFPs show how power can increase with
471 increased activation in the peaks, despite the low-level activation in the trough (Cii; triangle) that is
472 responsible for learning.

The same analysis has been performed for the recall condition after learning, with similar results. Importantly, the method of de-synchronisation is different in this condition. As Figure 7Di shows, in the NC an Alpha de-sync at recall is accompanied by a Theta sync, indicating that Alpha is de-synced by Theta as activation feeds into the Hippocampus, which in turn feeds activation back to the NC. This ensures we do not see a small synchronisation of Alpha with low levels of stimulus strength as we saw in the encoding condition. As Theta and Alpha phases are rarely aligned (as seen by comparing LFP plots in Figures 7Fi-ii), maximal Theta excitability is just as likely to de-synchronise by occurring during an Alpha inhibitory phase as it is to be facilitated by aligning with an Alpha excitatory phase. As stimulus strength increases, one observes both Hippocampal Theta synchronisation and NC Alpha desynchronisation accordingly, indicating that both are important for successful memory retrieval.

Figures 7E shows that the model is able to exhibit re-instantiation of a memory's content. That is, neo-cortical Alpha desynchronizes during recall for the stimulus cued, but not presented. This represents a purely endogenous activation of rich content.

Synch/De-Synch Predicts Learning

Having demonstrated that our model mimics the described behaviour of Alpha power decreases in the NC, and Theta power increases and phase dynamics in the Hippocampus, we now link these contrasting synchronisation behaviours with learning (see Figure 8). By varying the learning rate of STDP weight change (ε) between 0-1, it was possible to assess how the model behaves with different learning outcomes. The average of all bi-directional Hippocampal weights between subgroups P & NP increased with ε (Figure 8C), which is used here to assess learning, i.e. the stronger the weight change the better the memory. We then calculate the effectiveness of recall (P response to NP + NP response to P) as a percent change in power at a particular frequency from before learning to after learning, effectively allowing us to isolate the effect of learning on power. A bootstrap procedure then provided the confidence intervals (shaded area) around a mean (solid line) of recall power for incremental values of ε for pre-stimulus (black) and post-stimulus (red) periods.

From this we can use power at a particular frequency to predict whether learning has successfully occurred in our model, and vice versa. In respect of the sync/de-sync theory (Hanslmayr, et al., 2016), the model indicates that both a de-synchronisation of Alpha in NC areas (Figure 8Ai) and a synchronisation of Theta in Hippocampal areas (Figure 8Bi) during recall can predict successful memory retrieval.

Interestingly, one could also look at pre-stimulus Theta and Alpha power in the Hippocampus to predict whether learning has occurred (Figure 8Bi-ii ; black), where both increase by 30-40% due to stronger weights within the Hippocampus and reciprocal connectivity between the Hippocampus and NC. This is consistent with evidence that reports the importance of pre-stimulus Theta for learning (Gyderian, et al., 2009) (Fell, et al., 2011). The effect of feedback activity plays a smaller role in NC areas, where a small increase (<5%) in pre-stimulus Alpha power (Figure 8Ai; black) and an increase (<20%) in pre-stimulus Theta power (Figure 8Aii; black) can also predict learning (Salari & Rose, 2016). Importantly, there is a large synchronisation of Theta (<70%) at recall (Figure 8Bii; red) in NC areas, consistent with experimental findings (Burke, et al., 2014) (Klimesch, et al., 2005).

Discussion

We have presented a relatively simple spiking neural network model, which captures the complex synchronizing and desynchronizing behaviours of hippocampus and neocortex during encoding and retrieval in a typical memory task. This model, which we term the Sync/deSync (SdS) model, simulates hippocampal Theta synchronization and neocortical Alpha desynchronization in the service of encoding and retrieving novel stimulus associations – a key requirement of episodic memory. Consistent with the notion that one-shot learning occurs in the hippocampus, but not in the neocortex (O'Reilly, et al., 2014), our model only implements synaptic modifications in the hippocampus. This hippocampal learning uses two well-described synaptic modification mechanisms. The first is spike-timing-dependent-plasticity (Song, et al., 2000), where synaptic modifications increase exponentially with decreasing time lag between the firing of pre and post-synaptic neurons. The second mechanism

is Theta phase-dependent plasticity, where synapses between neurons firing in the inhibitory phase of Theta are strengthened, whereas synaptic connections between neurons firing in the excitatory phase are weakened (Hasselmo, 2005). In the model neo-cortex, neurons fire phase-locked to an Alpha oscillation when they receive no input (Jensen & Mazaheri, 2010) (Klimesch, et al., 2007). When these neurons are driven by a stimulus, they increase their firing rate and gradually desynchronize from the ongoing Alpha, especially when the input is strong enough to overcome maximum inhibition. Therefore, Alpha power decrease is negatively related to the neural firing rate (apart from the small power increase at low stimulus intensities), thereby mimicking the well-known negative relationship between Alpha and neural firing (Haegens, et al., 2011).

The Sync/deSync model draws inspiration from and resonates with a number of previous models that incorporate oscillations into the complementary learning systems framework. In particular, the concept of Theta phase-dependent plasticity in the Hippocampus has inspired aspects of a number of influential neural models (Hasselmo, et al., 2002) (Ketz, et al., 2013) (Norman, et al., 2005). An important component in two of these models (Hasselmo at al., 2005; Ketz et al., 2013) is a phase reversal between the two pathways from entorhinal cortex to CA1 (the monosynaptic performant pathway and the tri-synaptic pathway, via the schaffer collaterals), which could provide a powerful mechanism in terms of separating encoding from retrieval cycles. We chose not to fully model this aspect in detail, but focused particularly on the dynamics in area CA1 in order to keep the model as simple as possible. Norman et al. (2005) present an important refinement of the basic complementary learning systems model, in which the strength of k Winner-Take-All (kWTA) inhibition is varied across Theta phases. This modulation of inhibition provides a Theta-phase dependent learning, with parallels to the Sync/deSync model. That is, in the Norman et al. (2005) model, the high inhibition phase of Theta generates selective activation, restricting above-threshold activation to strongly responding units. LTP is then applied just to the active units, enabling selective weight update. This has similarities to the Sync/deSync idea that strongly active units move their spiking forward in the phase of Theta, enabling LTP (which only obtains in the inhibitory phase) to be selectively applied.

549 The match between the Norman et al and Sync/deSync models for the low inhibition phase of Theta
550 is a little weaker than for the high inhibition phase, but there are still parallels. Specifically, both
551 models exhibit activation of a broader profile of units in the low inhibition phase. In the Norman et al
552 model, this enables LTD to be applied to competitor units (that are not strongly tuned to the memory
553 being encoded). Sync/deSync similarly applies LTD in this low inhibition phase, however, it is a non-
554 specific, passive, decay.

555 Our use of an ADP function to reduce the capacity for units to spike multiple times in quick succession
556 is inherited from the Jensen & Lisman (2005) model. Additionally, while advancing the phase of Theta
557 at which a unit spikes plays a key role in the Sync/deSync model, it is somewhat different to precession
558 in the Jensen & Lisman model, where it encodes serial order.

559 The Sync/deSync model is also able to capture a number of human electrophysiological findings.
560 Human single neuron recordings revealed that hippocampal neurons can change their tuning, by
561 showing an increase in firing rate to a non-preferred stimulus after this stimulus has been associated
562 with a preferred stimulus (Ison, et al., 2015). Furthermore, Rutishauser et al. (2010) showed that a
563 significant portion of neurons in the MTL are phase-locked to the ongoing Theta rhythm during
564 memory encoding, with an increase in Theta phase-locking predicting later memory performance. Our
565 model is consistent with these findings in showing an increase in activation for newly associated
566 neurons, these responses being Theta phase-locked, and increased Theta synchronicity to be related
567 to later memory performance. However, Sync/deSync also suggests that responsive neurons during
568 learning are less locked to the ongoing Theta phase (Figure 4A and B), which seems at odds with
569 Rutishauser et al. (2010). This decrease in Theta phase-locking is present for responsive neurons only,
570 occurring since these units overcome maximum inhibition and thus fire at the LTP phase of Theta.
571 Importantly, Rutishauser et al. (2010) did not separate neurons into stimulus responsive (i.e. showing
572 an increase in firing rate) or not, therefore these findings cannot be directly linked to our model.
573 However, an interesting prediction that arises from the model is that the preferred phase of firing

differs between responsive and non-responsive neurons, and that this phase difference is related to later memory performance. Indeed, Rutishauser et al. (2010) found that different neurons were locked to different phases of ongoing Theta. In our model, this difference is most prominent when only the first spike occurring after maximum inhibition is considered, a specific prediction that can be tested in future experiments.

Inherent to the SdS model is that the same neurons can be either synchronised or de-synchronised depending upon the strength of driving input. By gradually increasing stimulus strength, a population with more inhibition/slower integration can exhibit a synchronisation at stimulus strengths when faster spiking populations exhibit a de-synchronisation (Figure 7B; ~10^5strength). This provides a neat explanation for the Sync/deSync conundrum, suggesting that it reflects the point where active neurons in different brain regions are on their trajectory towards a ceiling firing rate. We show in Figure 7B that the slower spiking hippocampal population synchronises with normal levels of input (~10^5, but will eventually de-synchronise (~10^6). In fact, non-invasive studies in humans have linked successful encoding of stimulus associations in the MTL with both Theta power increases (Kaplan, et al., 2012) (Staudigl & Hanslmayr, 2013) (Backus, et al., 2016), and decreases (Fellner, et al., 2016) (Crespo-Garcia, et al., 2016) (Greenberg, et al., 2015). SdS indicates that both eventualities could yield successful memory encoding (Figure 7B; black line & blue line, which is trending negative at the top range of stimulus strengths).

With respect to Alpha, many studies have shown that a decrease in Alpha power coincides with successful encoding and retrieval of episodic memories (see Hanslmayr et al., 2012; Hanslmayr & Staudigl, 2014 for reviews). In most previous studies, these effects extend also to beta. For this reason, and to ensure model simplicity, we have assumed only one cortical Alpha rhythm, we, though, see no reason why the same principles would not also apply to beta. During successful encoding of episodic memories, Alpha/beta power decreases have been found in left frontal areas for verbal material (Hanslmayr, et al., 2009) (Hanslmayr, et al., 2011) (Meeuwissen, et al., 2011) and occipital for visual

material (Noh, et al., 2014). During retrieval, Alpha/beta power decreases indicate the areas that are being reactivated, i.e. house the memory representation (Waldhauser, et al., 2016) (Michelmann, et al., 2016) (Khader & Rosler, 2011). This targeted Alpha/beta power decrease is exactly what is modelled here, with only neural assemblies that actively process the stimulus during encoding or retrieval showing power decreases, and the degree of this power decrease predicting memory performance. A key element of formal modelling is the identification of predictions that give the opportunity for the model to be falsified. The key predictions that SdS makes are presented in figure 7B, which shows that as driving stimulus strength increases, neo-cortical Alpha goes through an initial phase, (strength around 10^3), of Alpha power increase (i.e. synchronisation), followed by a much more marked Alpha power decrease (i.e. desynchronisation), which is maximal just below a strength of 10^5. This pattern could be argued to be inherent to the way synchronisation and desynchronization are modelled, i.e. a small increase in drive will generate more spikes at an oscillation's peak, and power will increase, while a large drive will cause spiking during the trough of the oscillation and power will go down. This pattern is our main prediction.

A further prediction is that the degree of Alpha power decrease should correlate with the degree of hippocampal Theta power increase, and the degree of phase precession of responsive neurons in the hippocampus. This prediction can be tested in intracranial EEG, which often records simultaneously from the neocortex and the hippocampus.

References

Andrade, R., 1991. Cell excitation enhances muscarinic cholinergic responses in rat association cortex. *Brain Resources,* pp. 81-93.

Araneda, R. & Andrade, R., 1991. 5-Hydroxtryptamine 2 and 5-hydroxtryptamine 1A receptors mediate opposing responses on membrane excitability in rat association cortex. *Neuroscience,* pp. 399-412.

Backus, A. et al., 2016. Hippocampal-prefrontal theta oscillations support memory integration. *Current Biology,* Volume 26, pp. 450-457.

Berger, H., 1929. Über das Elektrenkephalogramm des Menschen. *H. Archiv f. Psychiatrie,* 87(1), pp. 527-570.

627 Burke, J. F. et al., 2014. Theta and high-frequency activity mark spontaneous recall of episodic
628 memories. *Journal of Neuroscience,* 34(34), pp. 11355-11365.

629 Caesar, M., Brown, D. A., Gahwiler, B. H. & Knopfel, T., 1993. Characterization of a calcium-
630 dependent current generating a slow after depolarization of CA3 pyramidal cells in rat hippocampal
631 slice cultures. *European Journal of Neuroscience,* pp. 560-569.

632 Cohen, N. & Eichenbaum, H., 1993. *Memory, Amnesia, and the Hippocampal System.* s.l.:The MIT
633 Press.

634 Crespo-Garcia, M. et al., 2016. Slow-theta power decreases during item-place encoding predict
635 spatial accuracy of subsequent context recall. *NeuroImage,* 142(15), pp. 533-543.

636 Eichenbam, H., Yonelinas, A. P. & Ranganath, C., 2007. The medial temporal lobe and recognition
637 memory. *Annual Review Neuroscience,* Volume 30, pp. 123-152.

638 Fell, J. & Axmacher, N., 2011. The role of phase synchronisation in memory processes. *Nature Review*
639 *Neuroscience ,* Volume 12, pp. 105-118.

640 Fell, J. et al., 2011. Medial Temporal Theta/Alpha Power Enhancement Precedes Successful Memory
641 Encoding: Evidence Based on Intracranial EEG. *Journal of Neuroscience,* 31(14), pp. 5392-5397.

642 Fellner, M.-C.et al., 2016. Spatial Mnemonic Encoding: Theta Power Decreases and Medial Temporal
643 Lobe BOLD Increases Co-Occur during the Usage of the Method of Loci. *eNeuro,* 3(6).

644 Greenberg, J. A. et al., 2015. Decreases in Theta and Increases in High Frequency Activity Underlie
645 Associative Memory Encoding. *NeuroImage,* Volume 114, pp. 257-263.

646 Gyderian, S., Schott, B., Richardson-Klavehn, A. & Duzel, E., 2009. Medial temporal theta state
647 before an event predicts episodic encoding success in humans.. *PNAS,* 106(13), pp. 5365-5370.

648 Haegens, S. et al., 2011. α-Oscillations in the monkey sensorimotor network influence discrimination
649 performance by rhythmical inhibition of neuronal spiking. *PNAS,* 108(48), pp. 19377-19382.

650 Hanslmayr, S., Gross, J., Wolfgang, K. & Shapiro, K., 2011. The role of alpha oscillations in temporal
651 attention. *Brain Research Reviews,* pp. 331-343.

652 Hanslmayr, S., Spitzer, B. & Bauml, K.-H., 2009. Brain Oscillations Dissociate between Semantic and
653 Nonsemantic Encoding of Episodic Memories. *Cerbral Cortex,* 19(7), pp. 1631-1640.

654 Hanslmayr, S., Staresina, B. P. & Bowman, H., 2016. Oscillations and episodic memory: addressing
655 the synchronization/desynchronization conundrum. *Trends in Neuroscience,* 39(1), pp. 16-25.

656 Hanslmayr, S. & Staudigl, T., 2014. How brain oscillations form memories — A processing based
657 perspective on oscillatory subsequent memory effects. *NeuroImage,* 85(2), pp. 648-655.

658 Hanslmayr, S., Staudigl, T. & Fellner, M.-C., 2012. Oscillatory power decreases and long-term
659 memory: the information via desynchronization hypothesis. *Frontiers in Human Neuroscience.*

660 Hasselmo, M. E., 2005. What is the function of hippocampal theta rhythm? - Linking behavioral data
661 to phasic properties of field potential and unit recording data. *Hippocampus,* 15(7), pp. 936-949.

662 Hasselmo, M. E., Bodelon, C. & Wyble, B. P., 2002. A Proposed Function for Hippocampal Theta
663 Rhythm: Separate Phases of Encoding and Retrieval Enhance Reversal of Prior Learning. *Neural*
664 *Computation,* 14(4), pp. 793-817.

665 Hasselmo, M. E. & Eichenbaum, H. B., 2005. Hippocampal mechanisms for the context-dependent
666 retrieval of episodes. *Neural Networks,* 18(9), pp. 1172-1190.

667 Heusser, A. C., Poeppel, D., Ezzyat, Y. & Davachi, L., 2016. Episodic sequence memory is supported by
668 a theta-gamma phase code. *Nature Neuroscience ,* 19(10), pp. 1374-1380.

669 Huerta, P. T. & Lisman, J. E., 1995. Bidirectional synaptic plasticity induced by a single burst during
670 cholinergic theta oscillation in CA1 in vitro. *Neuron,* pp. 1053-1063.

671 Hughes, S. W. et al., 2004. Synchronized oscillations at alpha and theta frequencies in the lateral
672 geniculate nucleus.. *Neuron,* 42(2), pp. 254-68.

673 Huxter, J., Burgess, N. & O'Keefe, J., 2003. Independent rate and temporal coding in hippocampal
674 pyramidal cells. *Letters to Nature,* pp. 828-832.

675 Ison, M., Quiroga, R. & Fried, I., 2015. Rapid Encoding of New Memories by Individual Neurons in the
676 Human Brain. *Neuron,* Issue 87, pp. 220-230.

677 Jensen, O., Idiart, M. & Lisman, J., 1996. Physiologically Realistic Formation of Autoassociative
678 Memory in Networks with Theta/Gamma Oscillations: Role of Fast NMDA Channels. *Learning &*
679 *Memory,* pp. 243-256.

680 Jensen, O. & Lisman, J. E., 2005. Hippocampal sequence-encoding driven by a cortical multi-item
681 working memory buffer.. *Trends in neurosciences,* 28(2), pp. 67-72.

682 Jensen, O. & Mazaheri, A., 2010. Shaping functional architecture by oscillatory alpha activity: gating
683 by inhibition. *Frontiers in Human Neuroscience,* 4(186).

684 Jokisch, D. & Jensen, O., 2007. Modulation of Gamma and Alpha Activity during a Working Memory
685 Task Engaging the Dorsal or Ventral Stream. *Journal of Neuroscience,* 27(12), pp. 3244-3251.

686 Kaplan, R. et al., 2012. Movement-Related Theta Rhythm in Humans: Coordinating Self-Directed
687 Hippocampal Learning. *PLOS Biology.*

688 Ketz, N., Morkonda, S. G. & O'Reilly, R. C., 2013. Theta coordinated error-driven learning in the
689 hippocampus. *PLoS computational biology,* 9(6).

690 Khader, P. H. & Rosler, F., 2011. EEG power changes reflect distinct mechanisms during long-term
691 memory retrieval. *Psychophysiology,* Volume 48, pp. 362-369.

692 Khader, P., Jost, K., Ranganath, C. & Rosler, F., 2010. Theta and Alpha oscillations during working-
693 memory maintenance predict successful long-term memory encoding. *Neuroscience Letters,* 468(3),
694 pp. 339-343.

695 Klimesch, W., Barbel, S. & Sauseng, P., 2005. The Functional Significance of Theta and Upper Alpha
696 Oscillations. *Experimental Psychology,* 52(2), pp. 99-108.

697 Klimesch, W. et al., 1999. `Paradoxical' alpha synchronization in a memory task. *Cognitive Brain*
698 *Research,* 7(4), pp. 493-501.

699 Klimesch, W. et al., 2006. Oscillatory EEG correlates of episodic trace decay. *Cerebral Cortex,* Volume
700 16, pp. 280-290.

701 Klimesch, W., Sauseng, P. & Hanslmayr, S., 2007. EEG alpha oscillations: The inhibition–timing
702 hypothesis. *Brain Research Reviews,* 53(1), pp. 63-68.

703 Klimesch, W. et al., 1996. Event-related desynchronisation (ERD) and the Dm effect: does alpha
704 desynchronisation during encoding predict later recall performance?. *International Journal of*
705 *Psychology,* pp. 47-60.

706 Kumar, A., Rotter, S. & Aertsen, A., 2008. Conditions for Propagating Synchronous Spiking and
707 Asynchronous Firing Rates in a Cortical Network Model. *Journal of Neuroscience,* 28(20), pp. 5268-
708 5280.

709 Lega, B. C., Jacobs, J. & Kahana, M., 2012. Human hippocampal theta oscillations and the formation
710 of episodic memories. *Hippocampus,* Volume 22, pp. 748-761.

711 Libri, V., Constanti, A., Calaminici, M. & Nistico, G., 1994. A comparison of the muscarinic response
712 and morphological properties of identified cells in the guinea-pig olfactory cortex in vitro.
713 *Neuroscience,* pp. 331-347.

714 Mazaheri, A. & Jensen, O., 2005. Posterior α activity is not phase-reset by visual stimuli. *PNAS,*
715 103(8), pp. 2948-2952.

716 Meeuwissen, E. B., Takashima, A., Fernandez, G. & Jensen, O., 2011. Increase in posterior alpha
717 activity during rehearsal predicts successful long-term memory formation of word sequences.
718 *Human Brain Mapping,* pp. 2045-2053.

719 Michelmann, S., Bowman, H. & Hanslmayr, S., 2016. The Temporal Signature of Memories:
720 Identification of a General Mechanism for Dynamic Memory Replay in Humans. *PLoS Biology,* 14(8).

721 Noh, E., Herzmann, G., Curran, T. & de Sa, V. R., 2014. Using Single-trial EEG to Predict and Analyze
722 Subsequent Memory. *NeuroImage,* Volume 84, pp. 712-723.

723 Norman, K. A., Newman, E. L. & Perotte, A. J., 2005. Methods for reducing interference in the
724 complementary learning systems model: oscillating inhibition and autonomous memory rehearsal.
725 *Neural Networks,* 18(9), pp. 1212-1228.

726 O'Reilly, R. C., Bhattacharyya, R., Howard, M. D. & Kets, N., 2014. Complementary learning systems.
727 *Cognitive Science,* 38(6), pp. 1229-1248.

728 Pavlides, C., Greenstein, Y., Grudman, M. & Winson, J., 1988. Long-term potentiation in the dentate
729 gyrus is induced preferentially on the positive phase of θ-rhythm. *Brain Research,* 493(1-2), pp. 383-
730 387.

731 Pedreira, C. et al., 2010. Responses of Human Medial Temporal Lobe Neurons Are Modulated by
732 Stimulus Repetition. *Journal of Neurophysiology,* pp. 97-107.

733 Petsche, H., Stumpf, C. & Gogolak, G., 1962. The significance of the rabbit's septum as a relay station
734 between the midbrain and the hippocampus. I. The control of hippocampus arousal activity by the
735 septum cells.. *Electroencephalography Clinical Neurophysiology,* Volume 14, pp. 202-11.

736 Pfurtscheller, G., 2001. Functional brain imaging based on ERD/ERS. *Vision Research,* 41(10-11), pp.
737 1257-1260.

738 Rey, H. G., Fried, I. & Quiroga, R. Q., 2014. Timing of Single-Neuron and Local Field Potential
739 Responses in the Human Medial Temporal Lobe. *Current Biology,* pp. 299-304.

740 Rotstein, H. G. et al., 2005. Slow and fast inhibition and an H-current interact to create a theta
741 rhythm in a model of CA1 interneuron network. *J Neurophysiology,* 94(2), pp. 1509-18.

742 Rutishauser, U., Ross, I., Mamelak, A. & Schuman, E., 2010. Human memory strength is predicted by
743 theta-frequency phase-locking of single neurons. *Nature,* pp. 903-907.

744 Salari, N. & Rose, M., 2016. Dissociation of the functional relevance of different pre-stimulus
745 oscillatory activity for memory formation.. *Neuroimage,* Volume 125, pp. 1013-1021.

746 Sederberg, P. B. et al., 2003. Theta and gamma oscillations during encoding predict subsequent
747 recall. *Journal of Neuroscience,* pp. 10809-10814.

748 Sederberg, P. B. et al., 2007. Hippocampal and neocortical gamma oscillations predict memory
749 formation in humans. *Cerebrial Cortex,* pp. 1190-1196.

750 Song, S., Miller, K. D. & Abbot, L. F., 2000. Competetive Hebbian learning through spike-timing-
751 dependent-plasticity. *Nature Neuroscience.*

752 Staresina, B. P. et al., 2016. Hippocampal pattern completion is linked to gamma power increases
753 and alpha power decreases during recollection.. *eLife,* 10(5).

754 Staudigl, T. & Hanslmayr, S., 2013. Theta oscillations at encoding mediate the context-dependent
755 nature of human episodic memory. *Current Biology,* 23(12), pp. 1101-1106.

756 van Kerkoerle, T. et al., 2014. Alpha and gamma oscillations characterize feedback and feedforward
757 processing in monkey visual cortex. *PNAS,* 111(40), pp. 14332-41.

758 Waldhauser, G. T., Braun, V. & Hanslmayr, S., 2016. Episodic memory retrieval functionally relies on
759 very rapid reactivation of sensory information. *Journal of Neuroscience,* 36(1), pp. 251-260.

760 Waldhauser, G. T., Johansson, M. & Hanslmayr, S., 2012. Alpha/Beta Oscillations Indicate Inhibition
761 of Interfering Visual Memories. *Journal of Neuroscience,* 32(6), pp. 1953-1961.

762

763 ## Figure Legends

764 Figure 1: Experimental paradigm **(A)**. A non-preferred (NP) and preferred (P) image are found that the
765 neuron does not and does respond to. These are then combined and presented in a composite (C)
766 stimulus. Both P and NP images are presented again after this learning phase. Network connectivity
767 **(B)**. The architecture of the network **(Bi)** shows how a group of neo-cortical (NC) neurons and a group
768 of Hippocampal neurons receive input from a 10Hz and 4Hz tonic wave, respectively, and both groups
769 receive (background) noise from Poisson distributed spikes. Two subgroups of NC neurons receive
770 input from higher level areas that represent the P and NP image. Each subgroup of NC and Hip neurons
771 have reciprocal connectivity between themselves, 25% for NC and 40% for Hip. Hippocampal neurons
772 also receive an after-de-polarisation (ADP) function. Hippocampal neurons are interconnected (i.e.

773 not just within subgroups), again with 40% connectivity, and spike-time-dependent-plasticity (STDP)
774 is enabled with a Theta phase dependent learning rate **(Bii)**.

775 Figure 2: Hippocampal weight change throughout the simulation both within **(A)** and between
776 subgroups **(B)** that code for the P and NP stimulus. Weights within each subgroup increase when the
777 relevant image is presented **(A)**, where the magenta and blue periods indicate the presentation of the
778 NP and P images, respectively, and the green period indicates the presentation of both images
779 combined into a composite image. During this learning period, weights from the NP to the P subgroup
780 (magenta dashed) and vice-versa (blue solid) increase **(B)**. Outgoing weights then increase upon the
781 presentation of the relevant stimulus after learning (AL). Incoming weights also increase a small
782 amount before learning (BL), then decay back to zero.

783 Figure 3: Activity of Hippocampal neurons. Recognition reflects neurons responding to their own
784 stimulus, i.e. P units activating for the P stimulus. Cued recall reflects neurons responding to the
785 opposite stimulus, i.e. P units activating for the NP stimulus. Here, activation from before learning (BL)
786 **(A)**, after learning (AL) **(B)** and during learning (DL) **(C)** is shown. Raster plots show the activity of a
787 single P and NP neuron during presentations of the P stimulus BL **(Aiii)**, AL **(Biii)** and DL **(Ciii)**. The
788 average input into both P and NP neurons across all trials is shown in **Cii**, where coincidental external
789 drive (I_{ext}) during stimulus onset counteracts the effect of the ADP function (I_{ADP}). Additional activation
790 causes an increase in input from other neurons within the group (I_H) and also from the opposite group
791 ($I_{H<>H}$) as weights increase during learning. Smoothed activation data at recognition **(Di)** and recall **(Dii)**
792 is then compared to data reported in a MTL neuron study **(Diii)**.

793 Figure 4: Polar histograms for the recall condition of all spikes before **(Ai)**, during **(Bi)** and after learning
794 **(Ci)**, and of first spikes after -π/2 before **(Aii)**, during **(Bii)** and after learning **(Cii)**. **D** shows the
795 distinction between the excitatory (red) and inhibitory (green) phases of Theta, where LTD and LTP
796 occur, respectively.

797 Figure 5: Time-frequency-analysis (TFA) of Neo-Cortical Alpha for the recall and recognition conditions
798 before and after learning **(Ai-ii, Aiv-v)**, as well as during learning **(Aiii)**. A time-course of Alpha power
799 is shown for the colour-coded boxes around the recall condition before **(Ai)** and after **(Aiv)** learning,
800 where pure power **(Bi)** and percent change in pre-post stimulus power **(Bii)** are shown. The same
801 analysis can be seen for Hippocampal Alpha, where pure power **(Ci)** and relative power change **(Cii)**
802 are shown.

803 Figure 6: Time-frequency-analysis (TFA) of Hippocampal Theta for the recall and recognition
804 conditions before and after learning **(Ai-ii, Aiv-v)**, as well as for during learning **(Aiii)**. . A time-course
805 of Theta power is shown **(B)** for the colour-coded highlighted boxes **(Ai, Aiv)**, where pure power **(Bi)**
806 and percent change in pre-post stimulus power **(Bii)** are shown. The same analysis is shown for neo-
807 cortical Theta power during the same time periods **(Ci-ii)**.

808 Figure 7: Increasing stimulus strength (number of spikes being fed into NC neurons) during the
809 encoding (DL) and recall after learning conditions, where stimulus strength is depicted on a logarithmic
810 scale. During the encoding stage **(A-C)**, frequency by strength heatmaps of NC **(Ai)** and Hippocampus
811 **(Aii)** are shown. From this data, relative changes in NC Alpha **(B; red, 8-12Hz)** and Hippocampal Theta
812 power **(B; blue, 3-5Hz)** are plotted, as well as weight change between P and NP Hippocampal
813 subgroups **(B; black)**. From this plot, three different stimulus strength values are chosen: normal
814 oscillatory activity (~10^1 strength), small Alpha power increases (~10^3 strength) and maximal Theta
815 power increases (~10^5 strength). At these points, Local-field-potentials (LFPs) are calculated using
816 specific 2-6 or 8-12Hz filters for Hippocampal Theta **(Cii)** & NC Alpha **(Ci)**, respectively, where blue and
817 red highlighted regions indicate the possible stimulus onset area due to re-aligning phases across
818 multiple trials. The same symbols indicate at which point an LFP represents. The same format is
819 applied for the recall after learning condition **(D-F)**.

820 Figure 8: The effect of increasing the learning rate (ε), and therefore synaptic efficacy between P and
821 NP subgroups, on NC Alpha power **(Ai)**, Hippocampal Theta power **(Bi)**, NC Theta power **(Aii)** and

822 Hippocampal Alpha power **(Bii)**. **C** plots the mean and variance of P<->NP weights from 1000

823 simulations, where the learning rate (ε) was incremented gradually from 0 to 1.

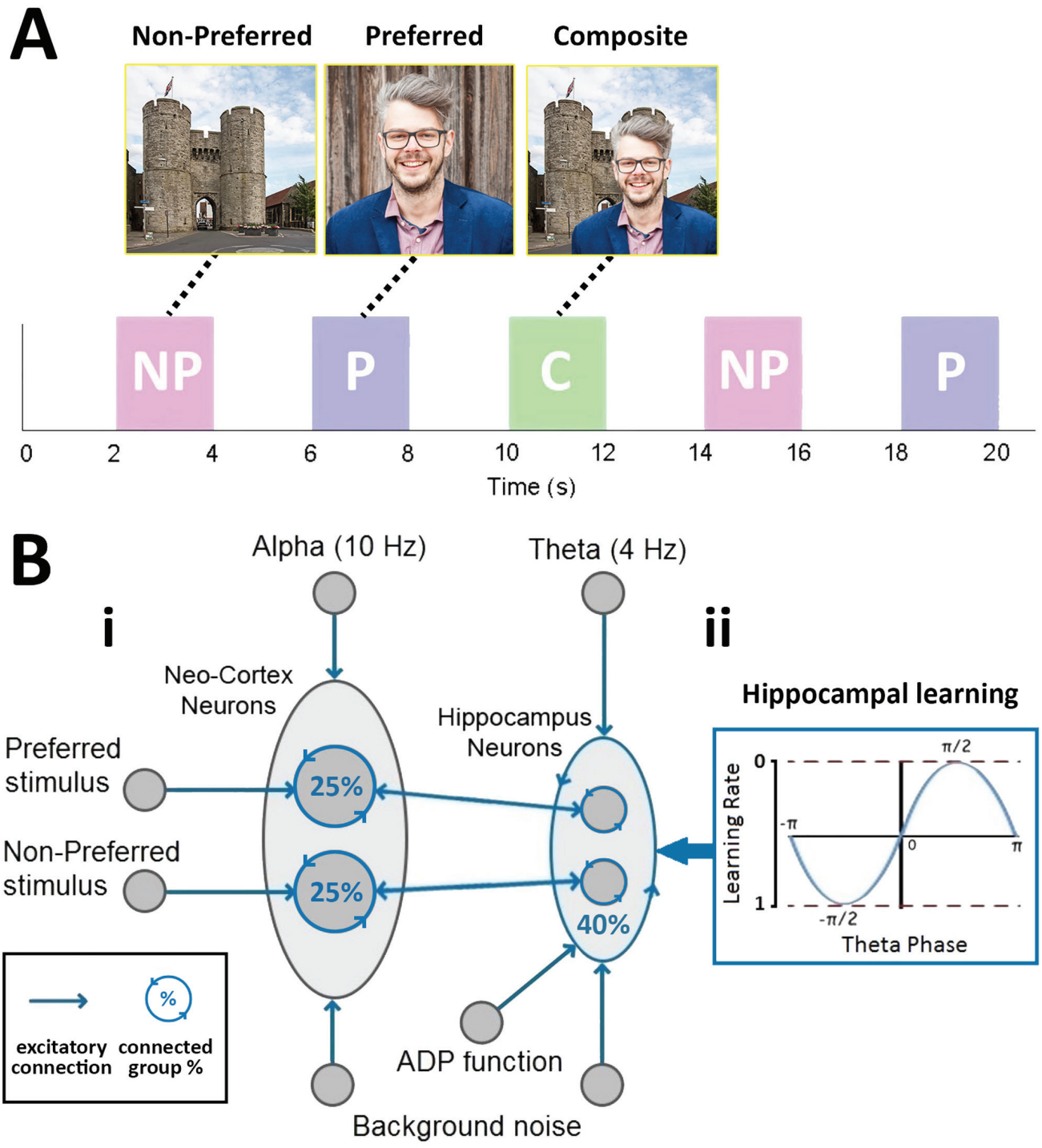

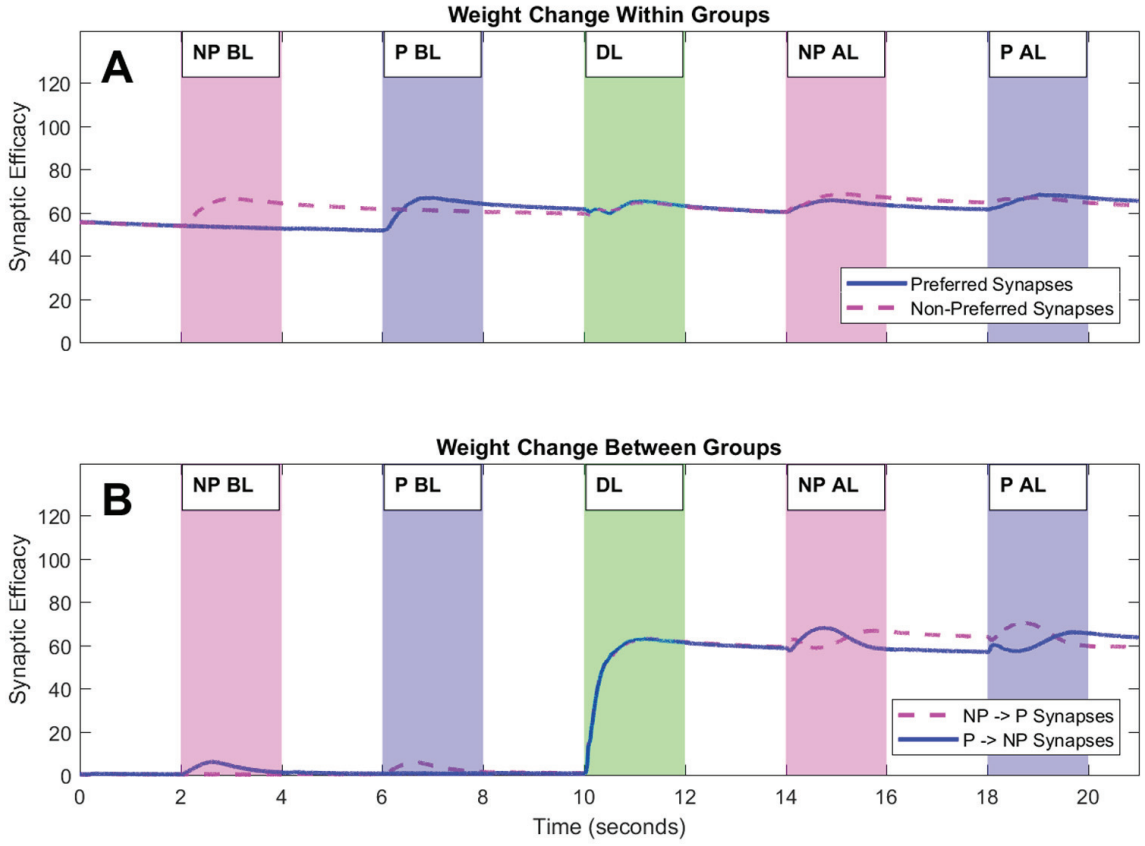

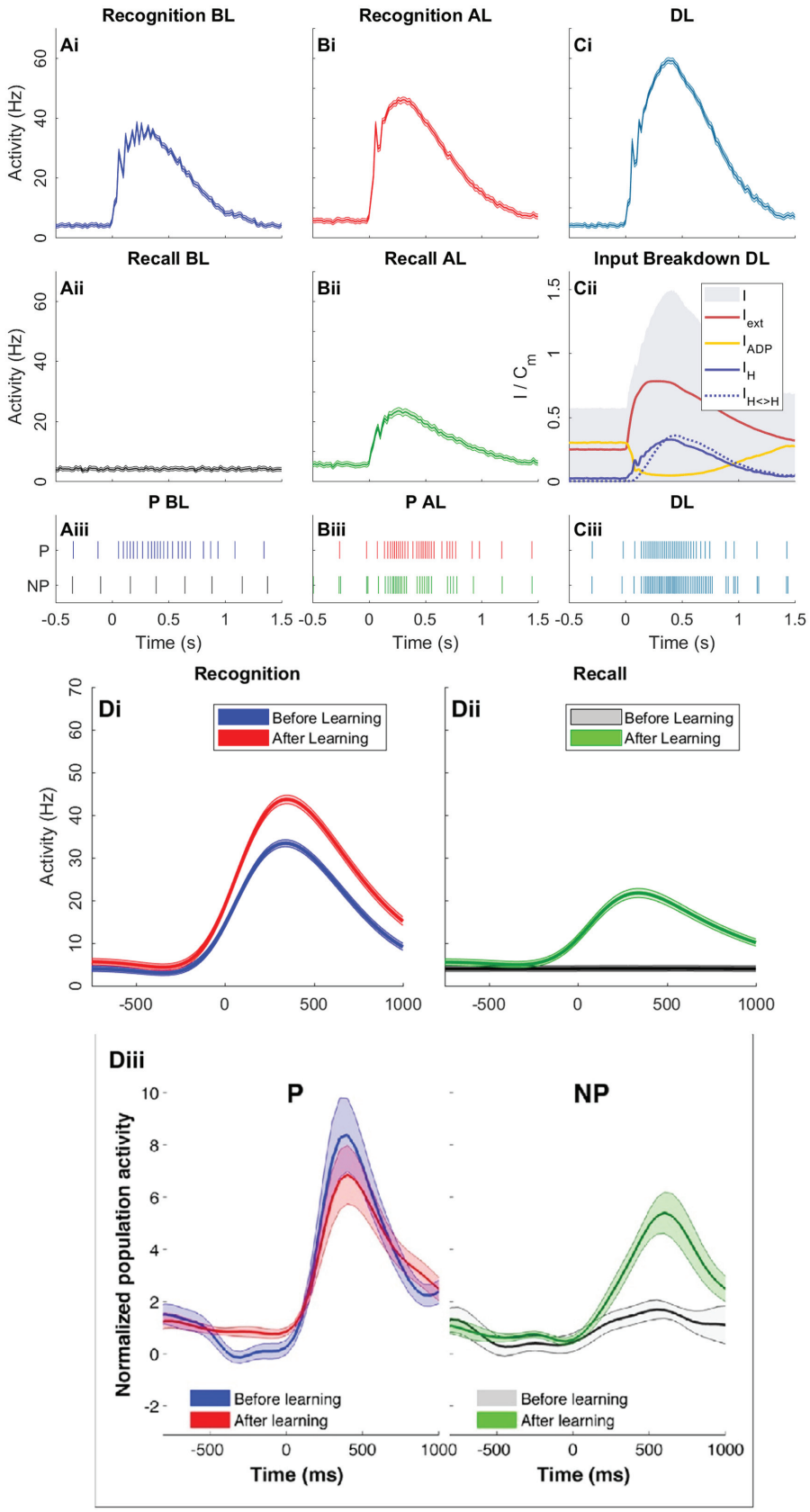

Rapid Encoding of New Memories by Individual Neurons in the Human Brain
Ison et al. 2015